Energy Storage Modeling of Inverter Air Conditioning for Output Optimizing of Wind Generation in Electricity Market

Meng Song, Ciwei Gao, Jianlin Yang, Huaguang Yan

Abstract—In order to achieve the compatibility of the air conditionings (ACs) loads with the current dispatch models, this paper utilizes demand response (DR) technology as energy storage resources to optimize the aggregator's behaviors in real-time market for less economic loss caused by the fluctuations of wind power. The inverter ACs as an typical demand response resource are constructed as the power type battery model (PTBM) and the capacity type battery model (CTBM) according to the different control ways, which are expressed through circuit model and mathematical model to describe the energy storage characteristics of ACs. Moreover, the comparisons between the PTBM and CTBM are given analytically in response speed, power &energy capacity and the cost of control, which will be helpful to guide the associated operators to choose appropriate models to take part in demand response. Considering that the wind generation fluctuates frequently and largely, the PTBM is chosen to take part demand response for output optimizing of wind generation. The simulation results demonstrate that PTBMs can work in the way of conventional batteries (CBs) to optimize wind generation in real-time market.

Index Terms—Demand Response, Inverter Air Conditioning, Energy Storage Modeling, Wind Generation, Electricity Market

I. INTRODUCTION

In recent years, the global wind power installed capacity continues to increase, and the annual growth rate is up to 28%[1]. Since 2005, China's wind power installed capacity continually improves. By the end of 2012, China's wind power installed capacity has reached 75.3GW, ranking at the first place in the world. However, due to the strong fluctuations of wind power, the prediction accuracy is low, which brings a series of problems to the security and stability of power grid and causes economic loss to the associated aggregators in electricity market. In order to promote large-scale wind power consumption and guarantee the economic benefit, energy storage technology has become one of the main ways to improve the wind power utilization rate [2-4]. Nevertheless, due to the high investment in energy storage equipment and the long cost recovery period, the further development of wind generation is seriously restricted.

Traditionally, end-users' loads are considered inelastic and only generators can be adjusted to keep supply-demand in a real-time balance. However, too frequent control times will increase mechanical stress on these generators [5]. And the increasing capacity of spare generators will cause huge waste due to the too little usage time. The rapid development of smart grid, especially the two-way communication technology and advanced measurement technology, will enable end users to receive real-time price information and communicate with the control center [6], which makes it possible to adjust end-users' loads. As one of the key technologies of smart grid, demand response (DR) has been widely utilized for the reason that it can relieve the tension of supply-demand unbalance, strengthen the grid dealing with power fluctuations and enhance the ability of the system to accommodate the renewable resources. Among all flexible loads, thermostatically controlled loads (TCLs) have received extensive attention by virtue of its ability to transfer loads at a certain time to provide a variety of ancillary services for the system [7, 8].

The energy consumption of residential and commercial buildings occupies up to 75% of total energy consumption of America [9], which makes TCLs become an important DR resource to take part in ancillary services. TCLs have been massively studied [10-12]. Ning Lu et al. [13] proposed a state-queuing model so as to describe the energy storage state of TCLs. Moreover, a general thermodynamic model has been developed concerning the evaluation of load shifting potential under different TCL control principles and electricity rate structures [14]. Ref. [15, 16] proposed a time-varying thermal battery model to keep track of the operating state of the TCLs. A simplified battery was developed in [17-19] to aggregate TCLs to provide frequency regulation service for the grid. Although battery models of TCLs have been studied in some literatures, these above-mentioned models are all limited to fixed frequency TCLs. The energy storage modeling of inverter ACs has been rarely studied.

Air conditionings (ACs) are the most typical and important part of TCLs. The compressors of ACs have evolved from fixed speed to variable speed units, which have gained noticeably growing market share for their higher energy efficiency [20，21]. At present, fixed frequency ACs are the main highlights in the majority of present literatures and there are many differences between fixed frequency and inverter ACs, which

M. Song, C. Gao are with the School of Electrical Engineering, Southeast University, Nanjing, Jiangsu 210096 China (corresponding author: +86-18905182095; e-mail: ciwei.gao@ 126.com). J. Yang is with Shanghai Power Company Economic Research Institute; H.Yan is with the China Electric Power Research Institute.

renders it impossible to model and control inverter ACs in the way of fixed frequency ACs. Therefore, this paper focuses on inverter ACs.

Generally, the fixed speed ACs can be controlled by on-off switches and the temperature set-point changes. Under different control methods, the fixed speed ACs will diversely operate in respond speed and power capacity [22]. Similarly, the inverter ACs can be controlled by frequency adjustment and temperature set-point changes. There are rare literatures that refer to the operating characteristics of the inverter AC under the two control methods. Therefore, two battery models of the inverter AC system are built in this paper.

The main contributions are as follows.

(1) The power type battery model (PTBM) of the inverter AC system with the frequency control (including circuit and mathematical model) is proposed, which shows the thermal energy storage behaviors of the AC and helps the AC be compatible with the current dispatch models. Furthermore, the aggregated model of heterogeneous PTBMs are built to make ACs scheduled conveniently;

(2) The capacity type battery model (CTBM) of the inverter AC with the temperature set-point change is also proposed. The differences between PTBM and CTBM in response speed, power capacity and the cost of control are analytically given, which will guide the associated operators to choose appropriate battery models to take part in demand response.

This paper is structured as follows. Firstly, the basic model of inverter AC system is introduced in chapter II. The PTBM of the inverter AC and the aggregated model of heterogeneous PTBMs are proposed in chapter III. In chapter IV, the CTBM is presented. The differences between the PTBM and CTBM are described in chapter V. The dispatch strategy of the aggregator in real-time market to reduce the economic loss is described in chapter VI. Case studies are given in chapter VII. Finally, chapter VIII summarizes the paper.

II. BASIC MODEL OF THE INVERTER AC SYSTEM

The inverter AC system model is composed of thermodynamic model and electrical model. A simplified equivalent thermal parameters (ETP) model [8] of a residential AC is described as (1). ETP model is well-suited for residential and small commercial buildings in the simulation of heat transition between the AC and its surroundings. There are two operating modes, namely heating and cooling mode for the AC and only the cooling mode is discussed in this context.

$$C_a \frac{dT_i}{dt} = \frac{1}{R}(T_o - T_i) + Q' - Q \tag{1}$$

where T_o is outdoor temperature, °C. T_i is indoor temperature, °C. C_a is the equivalent thermal capacity, kJ/°C. R is equivalent resistance, °C/kW. Q is the cooling power of inverter AC, kW. Q' is the internal heat generation power, kW.

The majority of power consumption of the inverter AC occurs during the compressor operation, whose coefficient of performance is not constant and varies with its rotational frequency. Hence, it is reasonable to consider the power consumption of the compressor as the total electric power of the

inverter AC. According to [20, 21], by further simplifications, the relationship between the frequency, f, and electric power, P, is expressed approximately as:

$$P = k_1 f + l_1 \tag{2}$$

where k_1 and l_1 are constant coefficients.

Similarly, Q is expressed as:

$$Q = k_2 f + l_2 \tag{3}$$

where k_2 and l_2 are constant coefficients.

According to (2) and (3), the relationship between P and Q is described as:

$$Q = \frac{k_2}{k_1} P + \frac{k_1 l_2 - l_1 k_2}{k_1} \tag{4}$$

The fundamental model of inverter AC system is composed of (1) and (4), which bridges the relationship between T_i and P. According to (2) and (3), it is clear that P can be continuously adjusted by the frequency control to provide services for the grid while keeping end-users in a comfort temperature range. In this way, the controller which is installed on the inverter AC is able to get power signals from associated dispatch centers and convert them into frequency signals to change the operating state of the compressor.

III. POWER TYPE BATTERY MODELING OF INVERTER ACs

In this section, the battery model of the AC is proposed when it is controlled by the frequency adjustment. The AC can change the electric power instantaneously and have large power capacity, which is similar to that of the power type conventional battery (CB). Thus, we name the model as PTBM under this control method.

A. The Circuit Model of the PTBM

When the inverter AC operates at the initial temperature set-point, $T_i(0)$, it is regarded that the AC is working in a natural state and the corresponding electric power is seen as the power baseline. From (1), the cooling power baseline, $Q_{baseline}$, is expressed as:

$$Q_{baseline} = \frac{1}{R}(T_o - T_i(0)) + Q' \tag{5}$$

According to (4), the electric power baseline, $P_{baseline}$, is given as:

$$P_{baseline} = \frac{k_1}{k_2 R}(T_o - T_i) + \frac{k_1 Q' + k_2 l_1 - k_1 l_2}{k_2} \tag{6}$$

Essentially, the AC is an electric device and cannot authentically charge or discharge. However, the indoor temperature that keeps end-users' comfortable is not a fixed value but a range [23], which makes it possible for the actual electric power P to deviate from $P_{baseline}$. When P is larger than $P_{baseline}$, the AC will absorb more electricity and it can be regarded as a charging process from the perspective of the grid. Similarly, when the actual electric power is smaller than $P_{baseline}$, it can be seen as a discharging process. Thus, the charging/discharging power of the PTBM, P_{cd}, is defined as [16]:

$$P_{cd} = P - P_{baseline} \tag{7}$$

According to the circuit theory, P is given as:

$$P = UI \tag{8}$$

where U is the voltage of the grid, V. I is the electric current, A.

From (4) and (8), (1) is rewritten as:

$$C_a \frac{dU'}{dt} + \frac{1}{R}U' + I' = I_1 \tag{9a}$$

$$U' = T_o - T_i \tag{9b}$$

$$I_1 = \frac{k_2 U}{k_1} I \tag{9c}$$

$$I' = \frac{k_1 Q' - k_1 l_2 + k_2 l_1}{k_1} \tag{9d}$$

The equivalent circuit model that is used to show the energy storage behaviors of the inverter AC system is given in Fig.1. The AC operates at the initial temperature set-point at the time 0. When P is increased by a larger frequency (i.e. $P_{cd}>0$), I will accordingly enlarge. From (9c), I_1 is determined by I and will also increase. Therefore, the electric current through C_a and R will go up and then U' will gradually become larger. Then there will be more energy stored in C_a and this is the dynamic charge process. Similarly, when P is reduced by a smaller frequency (i.e. $P_{cd}<0$), the electric current through R will decline and there will be an adverse electric current through C_a. U' slowly goes down and the stored energy in C_a is cut down. This is the dynamic discharge process.

In fact, according to the circuit model in Fig.1, it is also known that the electric power absorbed by the AC unit from the grid is consumed through three ways in the form of the thermal energy. The first one is to store thermal energy in the buildings ($C_a dU'/dt$). The envelope of the building and internal air work as a 'capacitance' to store the thermal energy. The second one is to make up the thermal dissipation because of the difference between the indoor and outdoor temperature (U'/R) and the third one is to take away the internal heat generation (I'). Due to the fact that the total dissipation power ($U'/R+ I'$) is much larger than that of the CB (the self-discharge power of the CB is very small and can be ignored), the AC needs to absorb much electricity to keep indoor temperature at the temperature set-point (i.e. make C_a constant). When the actual cooling power is larger than the dissipation power, more energy will be stored in the building (i.e. extra energy is stored in C_a). When the dissipation power is larger than the actual thermal power, the stored energy will decline ((i.e. some energy is released from C_a)). That is the physical principle of the energy storage of the AC system.
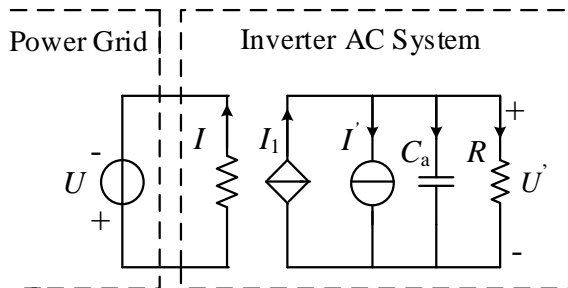

Fig. 1 Equivalent energy storage circuit model of the inverter AC system

B. The Mathematical Model of the PTBM

A CB can store electricity in the form of chemical or mechanical energy while the inverter AC system can store electricity in the form of thermal energy. To guarantee end-users' comfort, indoor temperature is kept within $[T_{min}, T_{max}]$. When indoor temperature is T_{min}, the stored energy is maximal while it is minimal when indoor temperature is T_{max}. It is assumed that the stored energy is 0 when indoor temperature is T_{max}. The state of charge (SOC) of the PTBM at time t is defined as:

$$SOC(t) = \frac{T_{max} - T_i}{T_{max} - T_{min}} \tag{10}$$

Substituting (10) to (1), the differential equation of SOC is expressed as:

$$\frac{dSOC(t)}{dt} = -\frac{1}{RC_a}SOC(t) - \frac{T_o - T_{max}}{RC_a(T_{max} - T_{min})} - \frac{Q' - Q}{C_a(T_{max} - T_{min})} \tag{11}$$

It is noted that the electric power of the inverter AC is kept constant during a dispatch period. Solve (11) and the formula about the SOC evolution is given by:

$$SOC(k+1) = e^{-\Delta t/RC_a} \cdot SOC(k) + \frac{R(1-e^{-\Delta t/RC_a})}{T_{max} - T_{min}} \cdot Q(k)$$
$$+ \frac{T_{max} - T_o - RQ'}{T_{max} - T_{min}}(1-e^{-\Delta t/RC_a}) \tag{12}$$

where $SOC(k+1)$ and $SOC(k)$ are the SOC at the $(k+1)^{th}$ and k^{th} period. $Q(k)$ is the cooling power of the AC at the kth period, kW.

According to (4) and (12), the relationship between the SOC and the electric power is described as:

$$SOC(k+1) = e^{-\Delta t/RC_a} \cdot SOC(k) + \frac{k_2 R(1-e^{-\Delta t/RC_a})}{k_1(T_{max} - T_{min})} \cdot P(k)$$
$$+ \frac{k_1(T_{max} - T_o - RQ') + R(k_1 l_2 - l_1 k_2)}{k_1(T_{max} - T_{min})}(1-e^{-\Delta t/RC_a}) \tag{13}$$

where $P(k)$ is the electric power of the AC at the kth period, kW.

From (7), (13) is rewritten as:

$$SOC(k+1) = \alpha SOC(k) + \beta P_{cd}(k) + \gamma \tag{14a}$$

$$\alpha = e^{-\Delta t/RC_a} \tag{14b}$$

$$\beta = \frac{k_2 R(1-e^{-\Delta t/RC_a})}{k_1(T_{max} - T_{min})} \tag{14c}$$

$$\gamma = (1-\alpha) \cdot SOC(0) \tag{14d}$$

$$SOC(0) = \frac{T_{max} - T_i(0)}{T_{max} - T_{min}} \tag{14e}$$

where $P_{cd}(k)$ is the charging/discharging power of the *PTBM* at the kth period, kW.

The evolution of the energy storage level with the charging/discharging power of the PTBM is described in (14a), which bridges the thermal energy and the electric energy in the form of the battery. This is a very important characteristic for the PTBM. Obviously, the SOC should be kept within the range [0, 1] to keep the end-users' comfort at any time. Then the constraint about SOC is given as:

$$0 \le SOC(k+1) \le 1 \tag{15}$$

At the same time, $P_{cd}(k)$ should be constrained as:

$$-P^d \leq P_{cd}(k) \leq P^c \qquad (16a)$$

$$P^d = P_{baseline} - P_{min} \qquad (16b)$$

$$P^c = P_{max} - P_{baseline} \qquad (16c)$$

where P_{min} and P_{max} are the minimum and maximum electric power of the inverter AC, kW, respectively.

To sum up, the PTBM of the inverter AC system can be described by (14a) (15) and (16a), which is identical with the expressions of the CB in [24-26].Therefore, the PTBM can replace the CB in the associated dispatch models, which makes the AC dispatched in the way of the CB and achieve the compatibility of the ACs with current dispatch models. For the system operator (SO), it might be familiar with the CB models and there have been many dispatch models developed for the batteries [27-29]. However, the model of the inverter AC system and its parameters are alien to the SO. Special revisions of the current dispatch model should be made to accommodate the ACs' participation. When the inverter AC is modeled as a conventional battery, the current dispatch model can be kept as it is, which brings a lot of convenience.

C. The Aggregation of Heterogeneous PTBMs

For the aggregator, it is hard to individually dispatch each PTBM from the perspective of the system and an aggregated model is necessary. The aggregated model of homogeneous PTBMs is built and then the heterogeneity of PTBMs is taken into account. It is obvious that only the heterogeneity of α and β need to be considered when the aggregated model of heterogeneous PTBMs is built according to the model of PTBM. Thus, the homogeneous PTBMs only have the same parameters $\{\alpha, \beta\}$.

The update of SOC of homogeneous PTBMs is calculated as:

$$\begin{cases} SOC_1(k+1) = \alpha SOC_1(k) + \beta P_1(k) + \gamma_1 \\ SOC_2(k+1) = \alpha SOC_2(k) + \beta P_2(k) + \gamma_2 \\ \vdots \\ SOC_m(k+1) = \alpha SOC_m(k) + \beta P_m(k) + \gamma_m \end{cases} \qquad (17)$$

where m is the number of PTBMs. $SOC_h(k+1)$ and $SOC_h(k)$ are the SOC of the hth ($1 \leq h \leq m$) PTBM at the $(k+1)^{th}$ and k^{th} period, respectively. $P_h(k)$ is the charging/discharging power of the hth PTBM at the kth period, kW. γ_h is the constant coefficient of the hth PTBM.

Aggregate the PTBMs and (17) is rewritten as:

$$\sum_{h=1}^{m} SOC_h(k+1) = \alpha \sum_{h=1}^{m} SOC_h(k) + \beta P_{agg}(k) + \sum_{h=1}^{m} \gamma_h \qquad (18a)$$

$$P_{agg}(k) = \sum_{h=1}^{m} P_h(k) \qquad (18b)$$

where $P_{agg}(k)$ is the aggregated charging/discharging power of the PTBMs at the kth period, kW.

In order to simplify the update of SOC in (18a), we introduce $SOC_{agg}(k)$ to describe the aggregated SOC of the PTBMs at the kth period. It is defined as:

$$SOC_{agg}(k) = \frac{\sum_{h=1}^{m} SOC_h(k)}{m} \qquad (19)$$

Then (18a) is rewritten as:

$$SOC_{agg}(k+1) = \alpha SOC_{agg}(k) + \kappa P_{agg}(k) + \sigma \qquad (20a)$$

$$\kappa = \beta / m \qquad (20b)$$

$$\sigma = \sum_{h=1}^{m} \gamma_h / m \qquad (20c)$$

Accordingly, $SOC_{agg}(k)$ in (19) should be constrained by:

$$0 \leq SOC_{agg}(k) \leq 1 \qquad (21)$$

Considering the charging/discharging power constraint of the PTBM in (16a), the aggregated charging/discharging power of PTBMs is given as:

$$-P_{agg}^d \leq P_{agg}(k) \leq P_{agg}^c \qquad (22a)$$

$$P_{agg}^d = \sum_{h=1}^{m} P_h^d \qquad (22b)$$

$$P_{agg}^c = \sum_{h=1}^{m} P_h^c \qquad (22c)$$

where P_h^d and P_h^c is the maximal discharging/charging power of the hth PTBM, kW, respectively.

The k-means algorithms [11] are employed to classify these heterogeneous parameters $\{\alpha, \beta\}$ of the PTBMs into n clusters and each cluster is associated with a center $\{\alpha^j, \beta^j\}(1 \leq j \leq n)$. It is regarded that PTBMs that falls into the same cluster have the same $\{\alpha^j, \beta^j\}$ and can be aggregated by the above modeling method.

Then the aggregated model of heterogeneous PTBMs is described as:

$$-D^{max} \leq P_n(k) \leq C^{max}$$
$$\boldsymbol{SOC}(k+1) = \boldsymbol{\alpha} \cdot \boldsymbol{SOC}(k) + \boldsymbol{\kappa} \cdot \boldsymbol{P}_n(k) + \boldsymbol{\sigma} \qquad (23)$$
$$0 \leq \boldsymbol{SOC}(k+1) \leq 1$$

where $C^{max} = \sum_{j=1}^{n} P_{agg}^{c\_j}$, $D^{max} = \sum_{j=1}^{n} P_{agg}^{d\_j}$, $P_n(k) = \sum_{j=1}^{n} P_{agg}^j(k)$,

$\boldsymbol{P}_n(k) = [P_{agg}^1(k), P_{agg}^2(k), \cdots, P_{agg}^n(k)]^T$, $\boldsymbol{SOC}(k) = [SOC_{agg}^1(k), SOC_{agg}^2(k), \ldots, SOC_{agg}^n(k)]^T$, $\boldsymbol{SOC}(k+1) = [SOC_{agg}^1(k+1), SOC_{agg}^2(k+1), \ldots, SOC_{agg}^n(k+1)]^T$. $\boldsymbol{\alpha} = [\alpha^1, \alpha^2, \ldots, \alpha^n]^T$. $\boldsymbol{\kappa}$ is a $n \times n$ matrix and its diagonal matrix is $[\kappa^1, \kappa^2, \ldots, \kappa^n]^T$. $\boldsymbol{\sigma} = [\sigma^1, \sigma^2, \ldots, \sigma^n]^T$. $P_{agg}^{c\_j}$ and $P_{agg}^{d\_j}$ are the maximal charging/discharging power of the PTBMs in the jth cluster, respectively. $P_{agg}^j(k)$ is the aggregated electric power of the PTBMs in the jth cluster, kW. $SOC_{agg}^j(k+1)$ and $SOC_{agg}^j(k)$ are the aggregated SOC of the PTBMs in the jth cluster at the $(k+1)^{th}$ period and k^{th} period. α^j, κ^j and σ^j are the aggregated constant parameters of the PTBMs in the jth cluster.

IV. CAPACITY TYPE BATTERY MODELING OF INVERTER ACs

In addition to the frequency control, the electricity consumption of the AC can also be changed by the adjustment of the temperature set-point. With the temperature set-point control, the AC cannot instantaneously reach the steady state but have huge energy capacity. Thus, the corresponding battery model is named as CTBM.

A. The Circuit Model of the CTBM

The charging/discharging process of the *CTBM* can also be described by Fig.1. Different from the frequency control, only the initial and final steady state are focused on and the transient

process of the indoor temperature fluctuations will be ignored if the dispatch period is long enough. When U' in Fig.1 reaches a lower set-point after the dynamic discharging process, U' will keep at the lower value for a long time until it is reset. And there is no electric current through C_a. Similarly, U' can keep at a larger value for a long time. It is obvious that once U' reaches the steady state after a dynamic charging/discharging process, the charging/discharging power will be constant, meaning that the CTBM will charge/discharge as long as U' is not re-modified. With this control method, the CTBM can be treated as a battery with a very huge energy capacity.

B. The Mathematical Model of the CTBM

When the AC is controlled by the temperature set-point modification, the frequency will be adjusted according to the difference between the actual and desired temperature until the indoor temperature reaches around the set-point. The frequency evolution is expressed as:

$$\Delta T = T_c - T_s \qquad (24)$$

$$f_{n+1} = \begin{cases} f_{max}, \Delta T > \Delta T_{max} \\ f_n + k\Delta T, -\Delta T_{min} \le \Delta T \le \Delta T_{max}, f_{min} \le f_{n+1} \le f_{max} \\ f_{min}, \Delta T < -\Delta T_{min} \end{cases} \qquad (25)$$

where T_s and T_c are the desired and the current temperature, ^oC. ΔT_{max} and ΔT_{min} are the maximum and minimum temperature error, which are determined by the AC, ^oC.

The charging/discharging power and SOC of the CTBM are defined identically with those of the PTBM in (7) and (10). Thus, the constraints of the charging/discharging power and SOC are also described by (16a) and (15).

According to (6) and (10), when the indoor temperature is kept constant, the relationship between P and SOC is given as:

$$P = \chi SOC + \varsigma \qquad (26a)$$

$$\chi = \frac{k_1(T_{max} - T_{min})}{k_2 R} \qquad (26b)$$

$$\varsigma = \frac{-k_1 T_{max} + k_1 RQ' + k_2 Rl_1 - k_1 Rl_2 + k_1 T_o}{k_2 R} \qquad (26c)$$

Due to the fact that SOC of the CTBM stay constant during the most time of the kth period, then the charging/discharging power of the CTBM at the kth period, $P_{CD}(k)$, is expressed as:

$$P_{CD}(k) = P(k) - P_{baseline} = \chi(SOC(k+1) - SOC(0)) \qquad (27)$$

It should be noted that $P(k)$ in (27) is the corresponding electric power when the indoor temperature reaches the steady state during the kth dispatch period.

Eq. (27) is rewritten as:

$$SOC(k+1) = \frac{1}{\chi} P_{CD}(k) + SOC(0) \qquad (28)$$

To sum up, the CTBM of the inverter AC system can be described by (15) (16a) and (28), which is also identical with the CB. The only difference among the three battery models (i.e. the CB, PTBM and CTBM) lies in the coefficients of the SOC update.

V. THE COMPARISONS OF THE PTBM AND CTBM

For the fact that the AC has different operating behaviors with the two control methods, the comparisons of the PTBM and CTBM are studies to guide the aggregators/operators to choose appropriate models to take part in demand response.

A. Response Speed

The parameters of the inverter AC system is given below. R, C_a and Q' are 2 ^oC/kW, 2kWh/^oC and 0.2kW, respectively. The other parameters are same as those in TABLE.III. The initial indoor temperature is 21 ^oC. T_{out} is 32 ^oC. Accordingly, the parameters of the PTBM are calculated in TABLE.I.

TABLE I
THE PARAMETERS OF THE PTBM

Parameter	α	β	γ	$P_{baseline}$	P^d	P^c
Value	0.8825	0.2350	0.0588	2.6	2.1	2.4
Unit	/	/	/	kW	kW	kW

PTBM works with the 0 charging/discharging power (i.e. AC operates at the initial temperature set-point) before the time 0.5 hour. Then it is controlled to charge/discharge and the corresponding charging/discharging power is 1.1, -2.1, 2.1, -2.1 kW, respectively. The dispatch period is 0.5 hour. The profiles of the actual electric power, SOC, and indoor temperature are shown in Fig.3. Due to the fact that the compressor of the AC can instantaneously respond the frequency signal to change the electricity consumption, the charging/discharging signals will be converted into frequency signals to immediately modify the operating state of the PTBM. Thus, the response speed of the PTBM is very fast and the charging/discharging power can be instantaneously obtained if the time delays of the communication and mechanics are ignored. At the same time, it is obvious that SOC of the PTBM is with an opposite varying tendency compared with indoor temperature, which means that the modeling method of PTBM is correct.
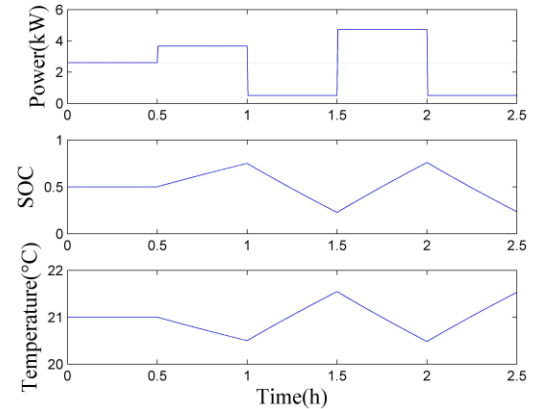

Fig.3 The profiles of the electric power, SOC and indoor temperatures of the PTBM

When the electricity consumption of the AC is adjusted by changing temperature set-point, the CTBM also keeps at the initial temperature point (21 ^oC) within the initial 0.5 hour. f_{min}, f_{max}, ΔT_{max}, ΔT_{min} and k are 30hz,180hz,3 ^oC,1 ^oC and 8, respectively. The dispatch period is 1 hour and the temperature set-point is adjusted to 21.5 and 20.5 ^oC, respectively. The evolutions of the actual electric power, SOC and indoor

temperature are shown in Fig.4. Obviously, it takes the AC a few minutes to make indoor temperature operate around set point, meaning that the respond speed of the CTBM is much slower than that of the PTBM and the CTBM is not suitable to be applied in such scenarios, in which, the dispatch period is short.
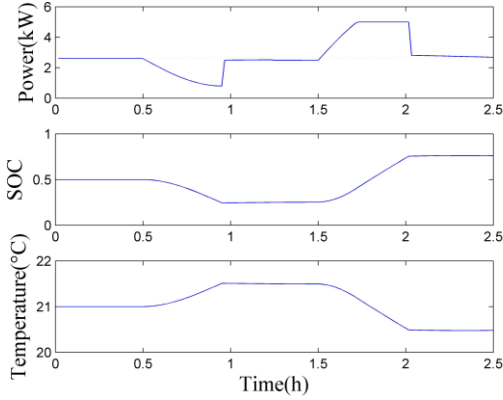

Fig.4 The profiles of the electric power, SOC, and indoor temperature of the CTBM

It should be noted that there is only one control signal during a dispatch period to change the electricity consumption. For the PTBM, the electric power determined by the frequency is fixed and cannot change with the varying outdoor temperature. Thus, the dispatch period should be short so that the variation of outdoor temperature is small and can be ignored. For CTBM, it can automatically modify the electricity consumption according to the varying outdoor temperature and keep the indoor temperature at the set-point. From this point of view, the CTBM is also more appropriate in the scenarios where the dispatch period is long.

B. Power & Energy Capacity

According to the definition of the PTBM in (14a) (15) and (16a), the maximum charging and discharging power (i.e. power capacity) of PTBM at the kth dispatch period, $P_{max}^P(k)$ and $P_{min}^P(k)$, are given as:

$$-P_{min}^P(k) \le P_{cd}(k) \le P_{max}^P(k) \quad (29a)$$

$$P_{min}^P(k) = \min(\frac{\alpha SOC(k)+\gamma}{\beta}, P^d) \quad (29b)$$

$$P_{max}^P(k) = \min(\frac{1-\alpha SOC(k)-\gamma}{\beta}, P^c) \quad (29c)$$

Similarly, the maximum charging and discharging power of the CTBM at the kth dispatch period, $P_{max}^C(k)$ and $P_{min}^C(k)$ are calculated as:

$$-P_{min}^C \le P_{CD}(k) \le P_{max}^C \quad (30a)$$

$$P_{min}^C = \min(\chi \cdot soc(0), P^d) \quad (30b)$$

$$P_{max}^C = \min(\chi \cdot (1-soc(0)), P^c) \quad (30c)$$

The maximum charging and discharging power profiles of the PTBM and CTBM under different dispatch periods are shown in Fig.5. For the PTBM, the maximum charging/discharging power keeps constant when the dispatch period is less about 0.5 hour. As the dispatch period increases, the maximum charging/discharging power become smaller.

Take the charging capacity as an example to explain the phenomenon. When the dispatch period is short, $(1-\alpha SOC(k)-\gamma)/\beta$ is larger than P^c and $P_{max}^P(k)$ is determined by the P^c. Then $P_{max}^P(k)$ keeps fixed. The power capacity is large and the energy capacity is small. When the dispatch period becomes longer, $(1-\alpha SOC(k)-\gamma)/\beta$ becomes less than P^c and $P_{max}^P(k)$ is determined by $(1-\alpha SOC(k)-\gamma)/\beta$. Obviously, $(1-\alpha SOC(k)-\gamma)/\beta$ will become less with the longer dispatch period. When the dispatch period approaches infinite, $(1-\alpha SOC(k)-\gamma)/\beta$ infinitely gets close to $k_1(T_{max}-T_{min})(1-SOC(0))/(k_2R)$ (i.e. $\chi(1-soc(0))$) and the energy capacity is also infinite.

By contrast, the power capacity of the CTBM is not affected by the dispatch period and it keeps fixed. It means that the CTBM can charge/discharge for a long time and can be seen as a battery with a huge energy capacity. This is because $\chi soc(0)$ is smaller than P^d and $P_{min}^C(k)$ is determined by $\chi soc(0)$. Similarly, $P_{max}^C(k)$ is determined by $\chi(1-soc(0))$. In other words, the power capacity of the CTBM is only related with $SOC(0)$. Due to the fact that it takes some time to adjust the indoor temperature reach the new set-point, the CTBM is not applied in the case that the dispatch period is short. It is also obvious that the power capacity of the PTBM is always larger than that of the CTBM. When the dispatch period approaches infinite, the power capacity of the PTBM infinitely closes to that of the CTBM. At this time, the PTBM can be approximately expressed by the CTBM in (15) (16a) and (28). The two models share similar operating behaviors and both of them have infinite energy capacity.
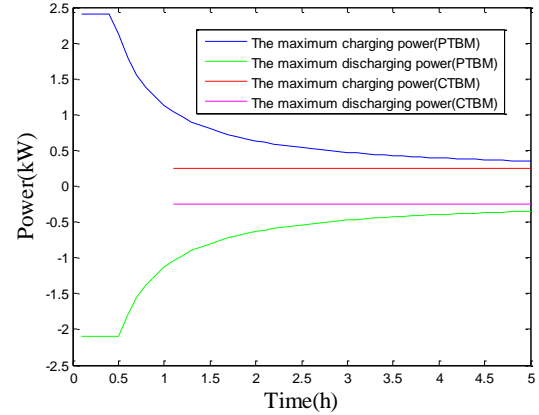

Fig.5 The capacity profiles of PTBM and CTBM under different dispatch period

C. The Cost of Control

Generally, the electricity consumption of the AC is modified by changing the temperature set-point. Then the frequency of the compressor is adjusted automatically to make the indoor temperature reach the set-point. If the AC is directly controlled by the frequency, some internal components of the AC need to be reformed or redesigned, which may bring huge expense. Thus, it is more convenient and cheaper for the AC to be controlled by changing of the temperature set-point compared with adjusting the frequency.

In a conclusion, the comparisons between the two models are summarized in TABLE. II.

TABLE.II

THE COMPARISONS BETWEEN THE PTBM AND CTBM

	Speed	Power Capacity	Energy Capacity	Cost
PTBM	fast	Large, related with the dispatch period	variable	much
CTBM	slow	small	large	little

Compared with the CTBM, the PTBM has faster response speed, larger power capacity but more cost. Thus, the PTBM is more suitable to be applied in some scenarios where the dispatch period is short and the response speed is fast (e.g. load following and frequency regulation) while the CTBM is more suitable to be applied in the scenarios where the dispatch period is long and there is no demanding need for the response speed (e.g. the load shaving). Although the power capacity of the PTBM is always larger than that of the CTBM, the CTBM has the advantage to take part in demand response because of its low control cost and huge energy capacity.

Considering the fact that the wind generation fluctuates frequently and largely, the PTBM is dispatched to optimize the output of wind generation. The applications of the CTBM will be studied in our future research.

VI. THE DISPATCH STRATEGY FOR OUTPUT OPTIMIZING OF WIND GENERATION

In this section, the PTBMs are dispatched to participate in real-time market for reducing the economic loss as a result of the fast fluctuations of the wind generation.

The aggregator that manages wind generation and loads is regarded as a single entity, which acts as a generator in the grid. In day-ahead electricity market, the aggregator submits its power generation schedule of the next day to the system operator (SO) in terms of its own wind power, load and electricity price forecasting, etc. SO receives the schedule information of all market players and the market clearing price is worked out according to the market rules [30]

Due to the great uncertainties of wind power, the difference between actual and the planned power of the aggregator is large, which may result in serious punishment and huge economic loss according to the market rules. Therefore, the aggregator needs to purchase/sell power in real-time market to reduce the losses when the power prediction is more accurate in the day.

In the real-time market, the scheduling of PTBMs are optimized to maximize the benefit of the aggregator. Two assumptions are made here: (1) the aggregator is a price-taker, its power is so small and has little impact on the price of real-time market; (2) the load is inelastic to electricity price. The MPC is to solve a finite-horizon optimization problem and only the first optimization operation is implemented [30]. The detailed optimization process is given as follows.

(1) Select a receding optimization period w and the forecast information of the wind generation, load and outdoor temperature in the future periods from $i+1$ to $i+w$ (i is the current dispatch period) are known. The maximum charge/discharge power of the PTBMs at the period from $i+1$ to $i+w$ can be obtained as well;

(2) Solve the optimization problem of the aggregator in real-time market. The objective function is to maximize the

economic income (or minimize the cost) [31, 32], which is a linear programming problem as:

$$\max F_c = \sum_{k=i}^{i+w} [(G(k) - P_n(k) - L(k) - Q(k)) p_{rt}(k)] \quad (31)$$

Subject to:

$$-D^{\max} \leq P_n(k) \leq C^{\max}$$
$$SOC(k+1) = \alpha \cdot SOC(k) + \kappa \cdot P_n(k) + \sigma$$
$$0 \leq SOC(k+1) \leq 1$$

where $Q(k)$ is the scheduled power of the aggregator in day-ahead market, MW. $G(k)$, $L(k)$ and $p_{ad}(k)$ are the predicted wind generation, load and electricity price, MW, MW, dollar/MW, respectively. w is the receding optimization period.

(3) Discharge/charge the PTBMs in terms of the optimization result of (31) at period $i+1$;

(4) Update the SOC of the PTBMs and move to the next period. Repeat the optimization process starting from step (1).

The optimization behaviors of the aggregator in the real-time market is described in Fig.6.
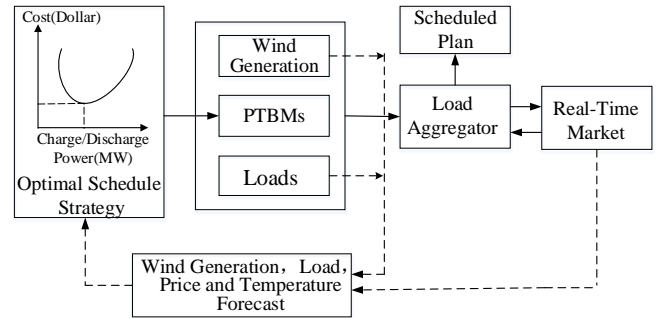

Fig.6 The behaviors of the aggregator in the real-time market

The aggregator develops optimal dispatch strategies of the PTBMs based on $SOC(k)$ and makes decisions on $P_n(k)$ according to the forecast of the wind generation, load, price and outdoor temperature. The control signals to PTBMs/ACs will be generated by the aggregator to change the electricity consumption. At the same time, $P_n(k)$ as the input of the aggregated model of the PTBMs is used to update $SOC(k+1)$ and proceeds to the next period. The control framework is shown in Fig.7.
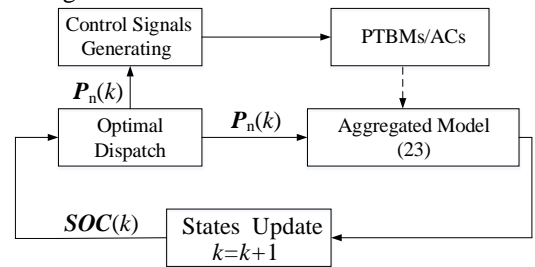

Fig.7 The control framework of the PTBMs

VII. CASE STUDIES

In this case, the number of inverter ACs is 2000 and their parameters are shown in TABLE. III. R, C_a, Q' and T_{set0} are all distributed randomly in their ranges. The dispatch period is 1 hour and the receding optimization period is 4. The simulation time is 24 hours. Wind generation, load and electricity price are

from [31-33]. The number of clusters is 10. We use the outdoor temperature provided by [34], which is a typical summer outdoor temperature profile in the region of PJM. During each dispatch period, outdoor temperature is regarded as a fixed value. The forecast method is from [31]. Considering that the fluctuations of the wind generation are much larger than those of loads and electricity price, only the uncertainties of the wind generation are taken into account.

TABLE III
THE PARAMETERS OF THE INVERTER AC SYSTEM

Parameter	Value	Unit
R	1.5-2.5	ºC/kW
C_a	1.5-2.5	kWh/ºC
Q'	0.1-0.5	kW
T_{set0}	20-22	ºC
T_{min}	20	ºC
T_{max}	22	ºC
P_{min}	0.5	kW
P_{max}	5	kW
k_1	0.03	kW/Hz
l_1	-0.4	kW
k_2	0.06	kW/Hz
l_2	-0.3	kW

A. The Optimization Results

The scheduled results of the aggregator in the day-ahead market is not the research point. For simplicity, $Q(k)$ is given as:

$$Q(k) = (G_a(k) - L_a(k)) \times (1 + v_d) \qquad (32)$$

where $G_a(k)$ and $L_a(k)$ are the actual wind generation and load at the kth period, MW, respectively. v_d is a rand number that is distributed uniformly in [-0.5,0.5]. The scheduled power, actual power and the power deviation (actual value-scheduled value) are shown in Fig.8. It can be seen that the difference between the scheduled power in day-ahead market and actual power is considerable because of the uncertainties of the wind generation. If the aggregator purchases/sells power according to the power deviation in real-time market in order to provide the scheduled power for the SO and not to be punished heavily, the aggregator will face huge risk of economic loss.
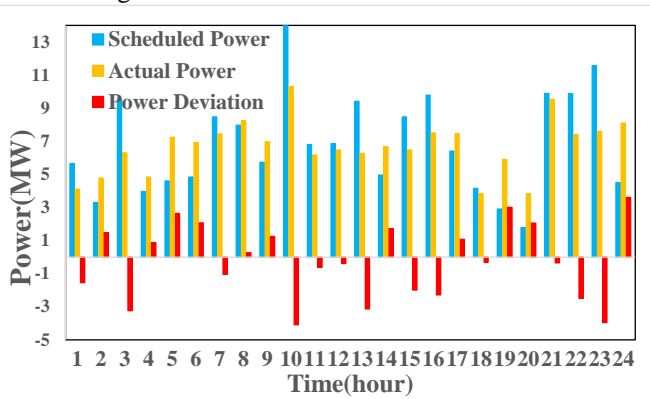

Fig.8 The comparisons of the scheduled power in day-ahead and the actual power

According to the parameters of the PTBM defined in (14b)-(14e) (16b) and (16c), it is obvious that only P^c and P^d are related with outdoor temperature ($P_{baseline}$ varies with outdoor temperature). The maximum aggregated charge power (i.e. C^{max} in (23)) and maximum aggregated discharge power (i.e. $-D^{max}$ in (23)) with varying outdoor temperature are shown in Fig.9. It can be seen that the maximum charge power decreases when the outdoor temperature rises and it will increase when the outdoor temperature drops. It means that the maximum charge power of PTBMs has an opposite changing tendency with outdoor temperature. Similarly, the maximum discharge power of PTBMs is with the same changing tendency of outdoor temperature. This is because that the baseline power of the PTBM (see (6)) has a positive linear relationship with outdoor temperature. When the outdoor temperature rises, the baseline power of the PTBM will increase, which will lead to a smaller charge power limit and a larger discharge limit according the definitions of the PTBM in (16b) and (16c).
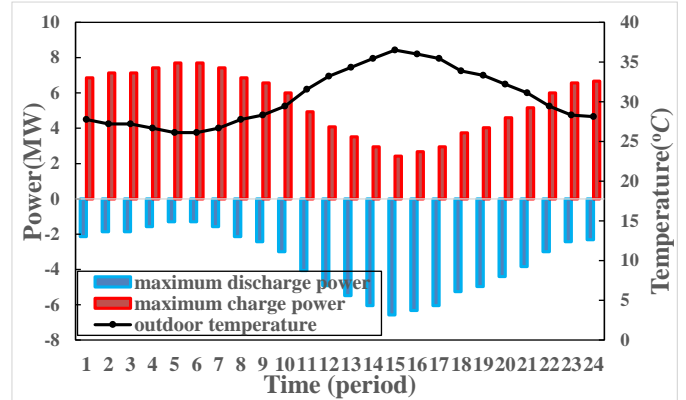

Fig.9 The maximum aggregated charge and discharge power of the PTBMs with varying outdoor temperature

Fig.10 shows the behaviors of the aggregator with two different strategies in real-time market. In strategy1, the aggregator without any energy storage devices purchases/sells electricity in real-time market according to the power mismatches between the actual wind generation and load. In strategy 2, the aggregator optimizes the charge/discharge power of PTBMs in real-time market for maximal economic benefit according to the dispatch model described in the Chapter VI. The income of the aggregator with the two strategies are -399 dollar and 1106 dollar, respectively. It means that the economic loss is 399 dollar when there is no energy storage devices while the income is 1106 dollar when the PTBMs are dispatched to optimize the behaviors of the aggregator. The PTBMs are beneficial to reduce the economic loss as a result of the fluctuations of the wind generation. The positive values of the aggregator mean that the aggregator sells electricity and the negative values mean that the aggregator purchases electricity in real-time market. It is obvious that the aggregator with PTBMs purchases more power at a lower price (e.g. the 3rd, 9th, 13th, 17th hour) and sells more power at a higher price (e.g. the 4th, 8th, 14th, 18th hour), which is similar to the operating way of the CBs. In other words, the PTBMs can replace the CBs in some dispatch frameworks. The PTBMs can make the aggregator operate more flexibly according to electricity price and provide the scheduled power for the SO.
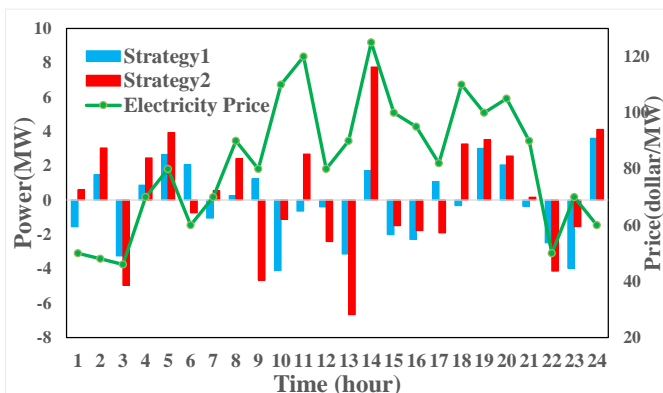
Fig.10 The optimization results of the aggregator with two strategies

B. The Impact of the End-users' Comfort Setting

This section focuses on the impact of temperature comfort level on the real-time scheduling results of the aggregator. The comparisons of real-time dispatch results of the aggregator under different temperature comfort levels are shown in Fig.11. The indoor temperature range of the level1，level2 and level3 in Fig.11 are $1\,^oC$ ([$20\,^oC$, $21\,^oC$]), $2\,^oC$([$20\,^oC$, $22\,^oC$]) and $4\,^oC$ ([$20\,^oC$, $24\,^oC$]), respectively. The income of the aggregator under the three comfort levels is 889, 1106 and 1356 dollar, respectively. As shown in Fig.11, the larger indoor temperature range can make the aggregator operate with more power potential. In other words, the aggregator with the wider temperature range will sell more power at the higher electricity price periods and purchases more power at the lower price periods. Although the sell/purchase power are both increased, the income of the aggregator is also increased because of the price difference. In a conclusion, the larger indoor temperature range allows PTBMs to be better at optimizing their behaviors in real-time scheduling for optimizing the fluctuations of the wind generation. However, this will also reduce users' comfort and cause more complaints, which will affect the enthusiasm of end-users to participate in demand response programs. Therefore, an appropriate temperature comfort level needs to be considered simultaneously in the signing of the agreement with end-users.
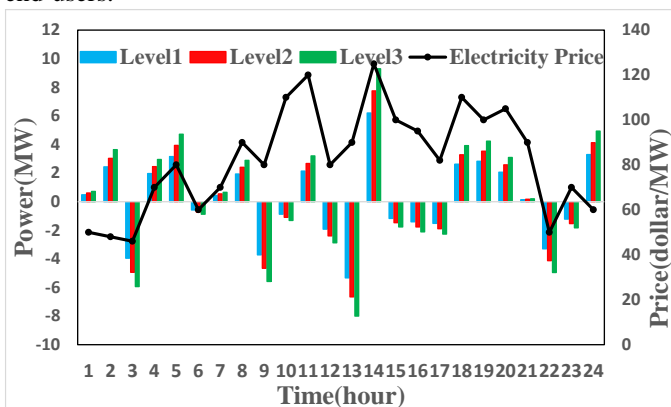

Fig.11 The behaviors of the aggregator under different end-users' comfort

VIII. CONCLUSIONS

In this paper, the inverter AC is constructed as an energy storage device model to optimize the behaviors of wind power in real-time market. Firstly, the circuit and mathematical model of the PTBM are established to show the energy storage characteristics of the inverter AC system. Secondly, for the comparison, the CTBM is also presented and the differences between the two models are given analytically. Thirdly, the PTBM is chosen to take part in real-time market in order to solve the problem of the fluctuations of the wind generation. The results are described as follows:(1) The inverter AC can be built as an energy storage model and have identically expressions with the CB because of its thermal energy storage characteristics, which helps the AC be compatible with the current dispatch models; (2) Compared with the CTBM, the PTBM has faster response speed, larger power capacity and more cost. Thus, the PTBM is more suitable to provide ancillary services where the dispatch period is short and the response speed is fast (e.g. load following and frequency regulation) while the CTBM is more suitable to take part in the demand response where the dispatch period is long and there is no demanding need for the response speed (e.g. the load shaving); (3) The PTBMs can help the aggregator to optimize its behaviors in real-time market for reducing the economic loss as a result of the uncertainties of the wind generation in the way of the CBs. The wider comfort level can make the aggregator work more flexibly.

Our future work will focus on new control strategies and algorithms to improve operation efficiency of PTBMs and CTBMs.

REFERENCES

[1] M. Yin, F. Han, J. Li, Y. Zhang, "Large-scale wind energy development in China and the relevant issues", IEEE PES/IAS Conference on Sustainable Alternative Energy, pp. 1-6, September 2009.

[2] C. Vartanian, N. Bentley, R. Foster, "Application of Advanced Battery Energy Storage Systems for Wind Integration", IEEE Power and Energy Society General Meeting, pp.22-26, July 2012

[3] C. N. Rasmussen, "Energy storage for improvement of wind power characteristics", *Proc. IEEE PowerTech*, pp. 1-8, Jun. 2011．

[4] B. C. Ummels, E. Pelgrum, W. L. Kling, "Integration of large-scale wind power and use of energy storage in the Netherlands' electricity supply", IET Renewable Power Gener., vol. 2, no. 1, pp. 34-46, Mar. 2008.

[5] N. Lu, D. Pengwei, Y. V. Makarov, "The potential of thermostatically controlled appliances for intra-hour energy storage applications", Proc. 2012 IEEE Power and Energy Society General Meeting, 2012-Jul.

[6] Y. Zhang, N. Lu, "Parameter selection for a centralized thermostatically controlled appliances load controller used for intra-hour load balancing", *IEEE Trans. Smart Grid*, vol. 4, no. 4, pp. 2100-2108, 2013．

[7] N. Lu, Y. Zhang, "Design considerations of a centralized load controller using thermostatically controlled appliances for continuous regulation reserves", *IEEE Trans. Smart Grid*, vol. 4, no. 2, pp. 914-921, 2013．

[8] N. Lu, "An evaluation of the HVAC load potential for providing load balancing service", *IEEE Trans. Smart Grid*, vol. 3, no. 3, pp. 1263-1270, 2012.

[9] Kelso, J.D., 2010 buildings energy data book. 2011: U.S. Dept. of

Energy.

[10] J. L. Mathiew, S. Koch, D. S. Callaway, "State estimation and control of electric loads to manage real-time energy imbalance", *IEEE Trans. Power Syst.*, vol. 28, no. 1, pp. 430-440, Feb. 2013

[11] W. Zhang, K. Kalsi, J. Fuller, M. Elizondo, D. Chassin, "Aggregate model for heterogeneous thermostatically controlled loads with demand response", Proc. IEEE PES General Meeting, 2012-Jul.

[12] A. Molina-Garca, M. Kessler, J. A. Fuentes, E. Gmez-Lzaro, "Probabilistic characterization of thermostatically controlled loads to model the impact of demand response programs", *IEEE Trans. Power Syst.*, vol. 26, no. 1, pp. 241-251, Feb. 2011.

[13] N. Lu, D. P. Chassin, "A state queuing model of thermostatically controlled appliances", *IEEE Trans. Power Syst.*, vol. 19, no. 3, pp. 1666-1673, Aug. 2004.

[14] J. Peppanen, M. J. Reno, S. Grijalva, "Thermal energy storage for air conditioning as an enabler of residential demand response", Proc. of North American Power Symposium (NAPS), pp.1-6,2014.

[15] M. Kamgarpour, C. Ellen, S. E. Z. Soudjani, S. Gerwinn, J. L. Mathieu, N. Mullner, A. Abate, D. S. Callaway, M. Fraenzle, J. Lygeros, "Modeling options for demand side participation of thermostatically controlled loads", *Proc. 2013 IREP Symp. Bulk Power System Dynamics and Control—IX Optimization Security and Control of the Emerging Power Grid (IREP)*, pp. 1-15, 2013

[16] J. Mathieu, M. Kamgarpour, J. Lygeros, G. Andersson, D. Callaway, "Arbitraging intraday wholesale energy market prices with aggregations of thermostatic loads", *IEEE Trans. Power Syst.*, vol. 30, no. 2, pp. 763-772, Mar. 2015.

[17] H. Hao, B. M. Sanandaji, K. Poolla and T. L. Vincent, "Aggregate flexibility of thermostatically controlled loads," IEEE Trans. Power Syst., vol. 30, no. 1, pp. 189-198, Jan. 2015.

[18] B. M. Sanandaji, H. Hao, K. Poolla and T. L. Vincent, "Improved battery models of an aggregation of thermostatically controlled loads for frequency regulation," *in Proc. 2014 American Control Conf.*, Portland, Jun. 2014, pp. 38-45..

[19] H. Hao, B. M. Sanandaji, K. Poolla and T. L. Vincent, "A generalized battery model of a collection of thermostatically controlled loads for providing ancillary service," in Proc. 2013 51st Annual Allerton Conference on Communication, Control, and Computing (Allerton), Monticello, IL, Oct. 2013, pp. 551-558.

[20] Y. J. Kim, L. K. Norford and J. L. Kirtley, "Modeling and analysis of a variable speed heat pump for frequency regulation through direct load control," IEEE Trans. on Power Syst., vol. 30, no. 1, pp. 397-408, Jan. 2015.

[21] Y. J. Kim, E. Fuentes and L. K. Norford, "Experimental study of grid frequency regulation ancillary service of a variable speed heat pump," *IEEE Trans. on Power Syst.*, vol. 31, no. 4, pp. 3090-3099, Jul. 2016.

[22] C. H. Wai, M. Beaudin, H. Zareipour, A. Schellenberg, N. Lu, "Cooling devices in demand response: A comparison of control methods", IEEE Trans. Smart Grid, vol. 6, no. 1, pp. 249-260, Jan. 2015.

[23] Chiguchi, Masao, et al. "Human thermal comfort estimation in indoor space by crowd sensing." Smart Grid Communications (Smart Grid Comm), 2016 IEEE International Conference on. IEEE, 2016.

[24] H. Xing, M. Fu, Z. Lin and Y. Mou, "Decentralized optimal scheduling for charging and discharging of plug-in electric vehicles in smart grids," *IEEE Trans. Power Syst.*, vol. 31, no. 5, pp. 4118-4127, Sep. 2016.

[25] C. Shao, X. Wang, X. Wang, C. Du and B. Wang, "Hierarchical charge control of large populations of EVs," *IEEE Trans. Smart Grid*, vol. 7, no. 2, pp. 1147-1155, Mar. 2016.

[26] D. Wang, X. Guan, J. Wu, P. Li, P. Zan and H. Xu, "Integrated energy exchange Scheduling for multi micro grid system with electric vehicles," *IEEE Trans. Smart Grid,* vol. 7, no. 4, pp. 1762-1774, Jul. 2016.

[27] Y. Wen, W. Li, G. Huang and X. Liu, "Frequency dynamics constrained unit commitment with battery energy storage," *IEEE Transactions on Power Systems*, vol. 31, no. 6, pp. 5115-5125,

Nov. 2016.

[28] M. T. Zareifard, "Model predictive control of electricity market oriented wind farm dispatch with a battery energy storage system," *in Proc. IEEE Conf. on Control Appl. (CCA),* Sydney, NSW, Sep. 2015, pp. 727-732.

[29] N. Piphitpattanaprapt and D. Bangerdpongchai, "Optimal dispatch strategy of hybrid power generation with battery energy storage system in islanding mode," *in Proc. IEEE Conf. Smart Grid Tech. - Asia (ISGT ASIA)*, Bangkok, NSW, Nov. 2015, pp. 1-6.

[30] Y. Xu and C. Singh, "Adequacy and economy analysis of distribution systems integrated with electric energy storage and renewable energy resources," *IEEE Trans. Power Syst.*, vol. 27, no. 4, pp. 2332-2341, Nov. 2012.

[31] Y. Xu and C. Singh, "Operation strategies of the load aggregator with electric energy storage," *in Proc. IEEE. Int. Conf. Power Syst. Technol. (POWERCON)*, Auckland, USA, Oct. 2012, pp. 1-6.

[32] Yixing Xu, Le Xie and Chanan Singh, "Optimal scheduling and operation of load aggregator with electric energy storage in power markets," *in Proc. North American Power Symposium 2010*, Arlington, TX, 2010, pp. 1-7.

[33] M. S. Kang, C. S. Chen, Y. L. Ke, C. H. Lin and C. W. Huang, "Load profile synthesis and wind-power-generation prediction for an isolated power system," *IEEE Trans. Ind. Appl.*, vol. 43, no. 6, pp. 1459-1464, Nov./Dec. 2007.

[34] E. Anastasio (2017, Jan. 10). Load Forecasting at PJM [Online]. Available: http://www.pjm.com/~/media/committees-groups/committees/oc/20170110/20170110-item-06-load-forecasting-at-pjm.ashx

Meng Song received her M.Eng degree in Electrical Engineering from Harbin Institute of Technology, Harbin, China, in 2014. She is currently pursuing a Ph.D. degree in Electrical Engineering at Southeast University, China.
Her research interests include demand side management, modeling and analysis of HVAC

Ciwei Gao received his M.Eng degree in Electrical Engineering from Wuhan University, Wuhan, China, in 2002. He received his Ph.D. degree in Electrical Engineering from Shanghai Jiaotong Univertisty, China, and Polytecnico di Torino,Italy, in 2006. He is now a professor in the School of Electrical Engineering, Southeast University, China. His research interests include electricity market, demand side management and power system planning.

Jianlin Yang received his B.Sc., M.Sc. and Ph.D. degrees, all in Electric Engineering, from South China University of Technology, Guangzhou in 2003, Tianjin University, Tianjin in 2006, and Shanghai Jiao Tong University, Shanghai in 2010, respectively. He is currently senior engineer in Shanghai Economic Technology Research Institute. His research interests include power grid planning, deregulation of electric energy industry, and stability analysis of power systems.

Huaguang Yan received his M.Eng degree in Electrical Engineering from Wuhan University, Wuhan, China, in 2003. He is now the chief engineer in electricity using and efficiency department of China Electric Power Research Institute. His research area includes demand side management and smart power utilization